

Supplemental figure legends

Supplemental figure 1. Refined analysis and confirmation of the observed interactions (A-B) The PLP binding domain of profilin might not be the only binding site for the GPR loop. GST-GPR coupled beads were incubated with wild-type or profilin mutant lysates and successively washed with 100 μ M PLP and 1M NaCl. Profilin mutants are profilin I and II (PI/PII) double knockout, complemented with versions of profilin II bearing targeted substitutions (Lee et al, 2000). The point mutant W3N is abolished in PLP binding and slightly impaired in actin binding while the point mutant K114E is abolished in actin binding but has intact PLP binding activity. GPR binding of both constructs could be disrupted by PLP elution although the W3N profilin II variant is not supposed to bind to PLP anymore. The W3N variant was retained on the GST-GPR beads after PLP elution but was detached at high salt. Therefore, interaction of profilin II with the GPR loop might be mediated not only by poly-Pro stretches but also by unconventional ZPP ϕ motifs and electrostatic interactions. (C) More Arp3 is eluted together with Abp1 by PLP from GST-GPR beads than from GST-PRD beads. GST beads were used as negative control. (D) A fraction of Abp1 and actin co-purifies with MyoK after two chromatographic separation steps of a myosin enriched fraction. Cell lysates of MyoK OE (MyoK) were used to obtain a myosin enriched fraction by ATP release from an actin pellet. Higher purity was obtained by expressing a His-tagged MyoK construct (K824) with an intact motor domain and GPR loop but with two actinin repeats (2R) fused directly to the motor domain at residue 824. K824-2R was purified in a similar manner as MyoK. After ATP release, this fusion protein was further purified by chromatography. (*left panel*) Ponceau staining of the blotted fractions. MyoK full length and K824-2R are indicated by asterisks in the corresponding lanes. Arrowhead points at actin. (*right panel*) The purification steps of a MyoK construct were analyzed by immunoblotting for the presence of myosin II, Abp1 and Arp3. Myosins were significantly enriched after ATP release. Actin and Abp1 co-fractionated with MyoK while Arp3 did not, corroborating that it might interact only indirectly with MyoK. (E-F) Blot overlays showing the direct interaction of the GST-GPR loop with immobilized Abp1. A weak interaction of the GPR loop with dynamin A is detected.

Supplemental figure 2. Experimental SPR curves of data presented in Table I. Absence of binding of GST-PRD to immobilized GST-Abp1 confirms results of blot overlays and demonstrates that measurement of potential GST-GST interactions are negligible and efficiently subtracted (A). SPR experimental binding curves of GST-GPR to immobilized profilin I (B) and profilin II (C) or GST-GPR (D) to immobilized GST-GPR.

Supplemental figure 3. MyoK and Abp1 have differential temporal profiles during early steps of phagosome maturation. Immunoblots of latex bead phagosomes purified after the indicated period of pulse. In order to shed light on the mechanism of uptake, we examined the content of phagosomes purified at very short intervals (2 to 12 minutes) during ingestion. Detailed temporal profiling revealed a difference in the recruitment of MyoK and Abp1 that correlated with an early and late phase of actin dynamics. MyoK, profilin and myosin II were transiently enriched on 2 to 6 min phagosomes, while actin and Abp1 were also present early but dissociated later. Dynamin A, another binding partner of Abp1, displayed a distinct but intermediate dissociation kinetics compared to the two groups of actin-associated proteins. Early markers of membrane delivery such as the subunit A of the vacuolar H⁺-ATPase (VatA) and the lysosomal membrane protein B (LmpB) continuously increased until 12 min, as expected from longer pulse/chase experiments (Gotthardt *et al.*, 2002) and validated the specificities of the other recruitment profiles.

Supplemental figure 4. Scenarios. This figure repeats the schematic model of the MyoK-Abp1-PakB circuit (Figure 7G) and presents explicitly the impact on phagocytosis of the combinations of gene ablations and complementations described in this study. The increases/decreases are indicated intuitively by thicker/thinner lines or bolder/thinner characters, respectively.

Supplemental figure 5. Sequence analysis of *Dictyostelium* Abp1, WASp and dynamin A.

Figure S1
Dieckmann et al

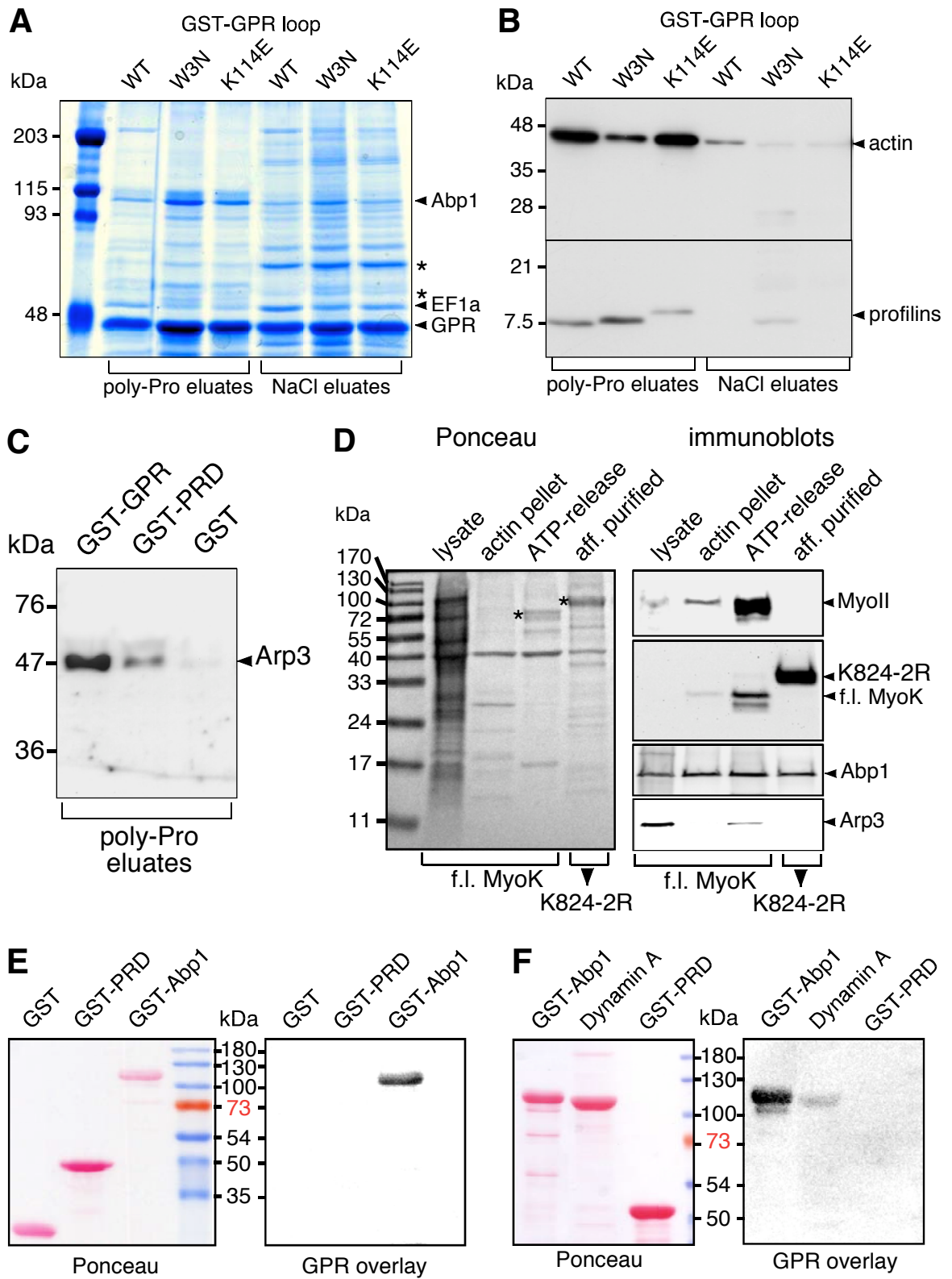


Figure S2
Dieckmann et al

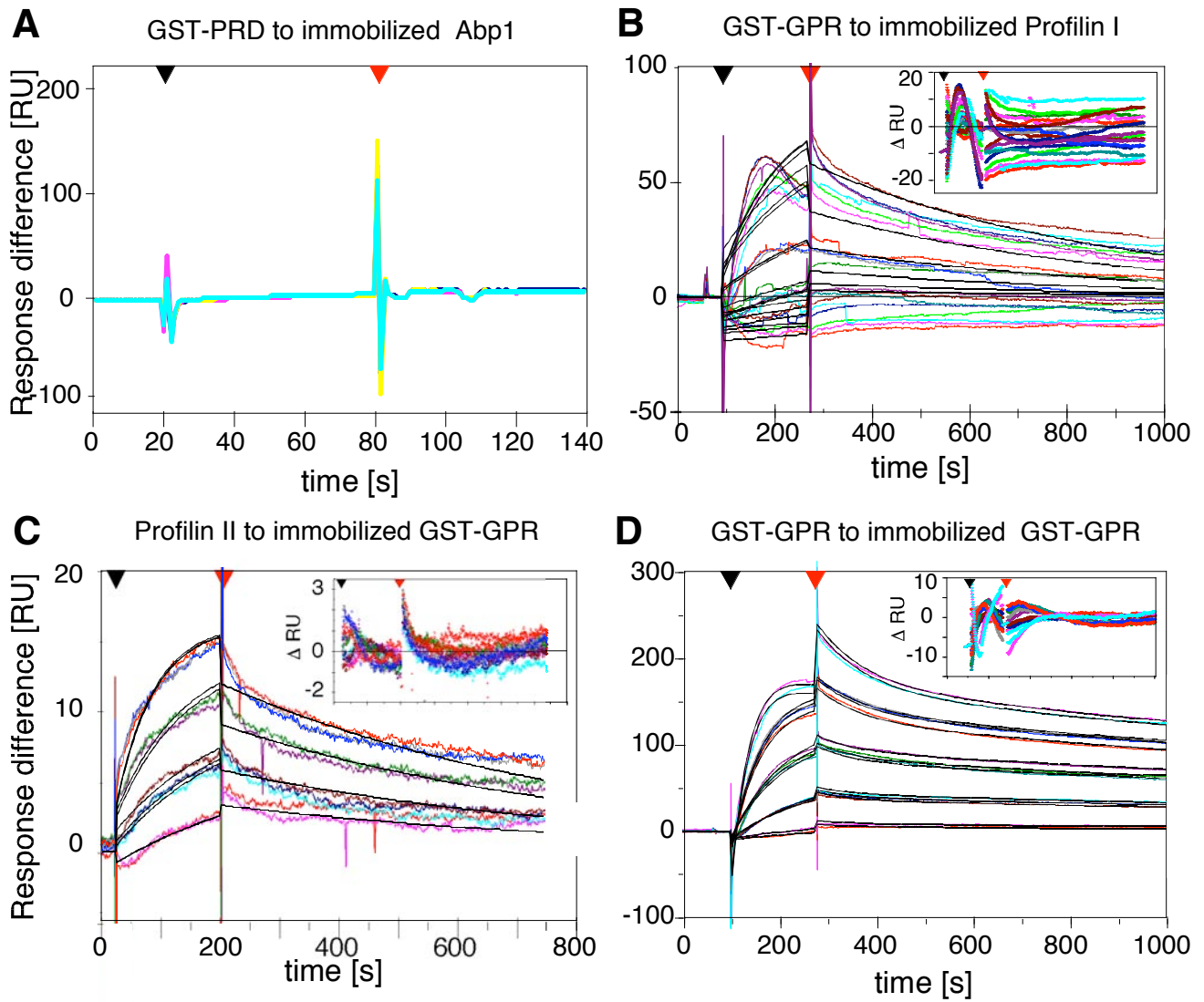


Figure S3
Dieckmann et al

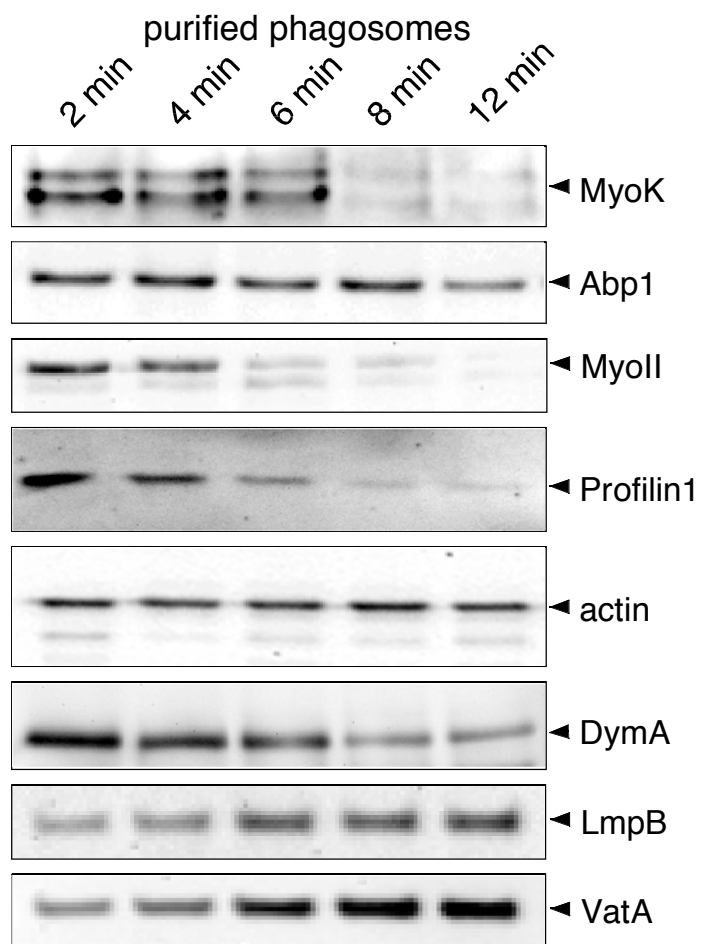
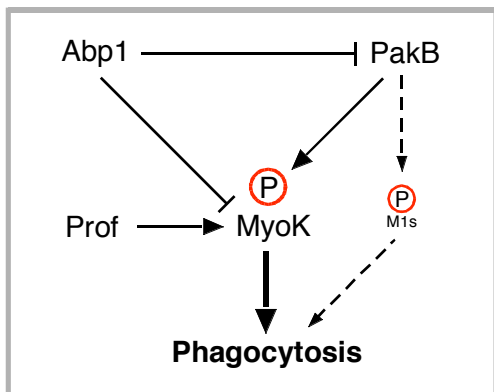
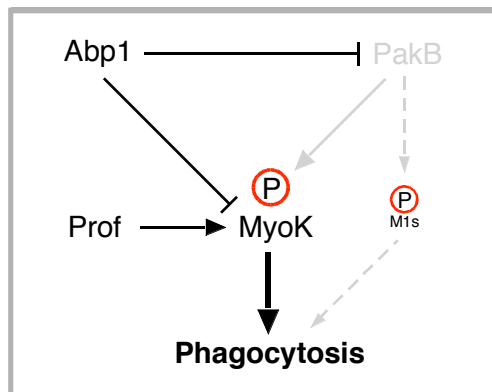


Figure S4
Dieckmann et al

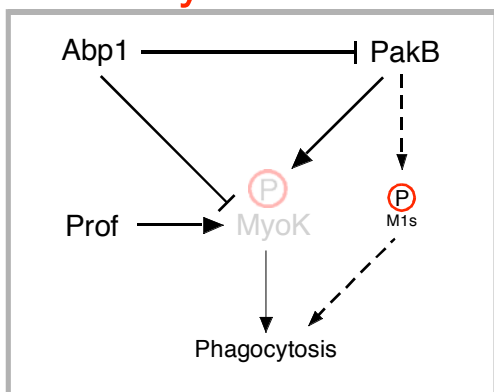
WT



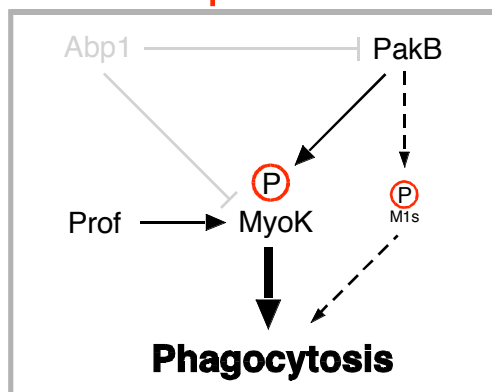
PakB null



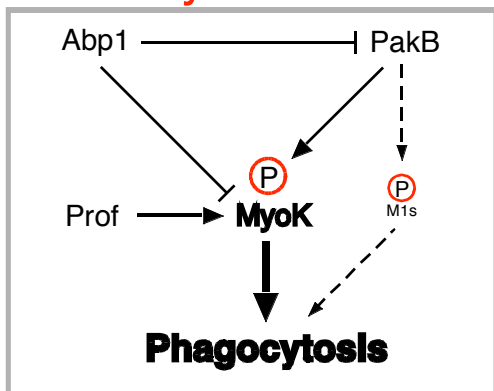
MyoK null



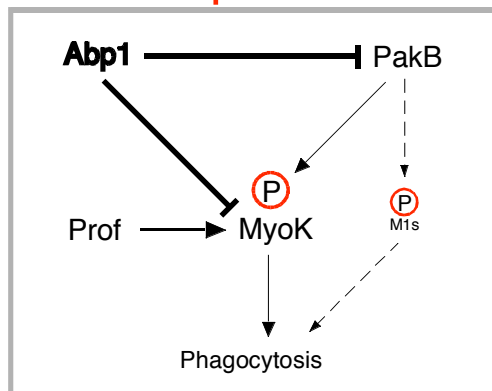
Abp1 null



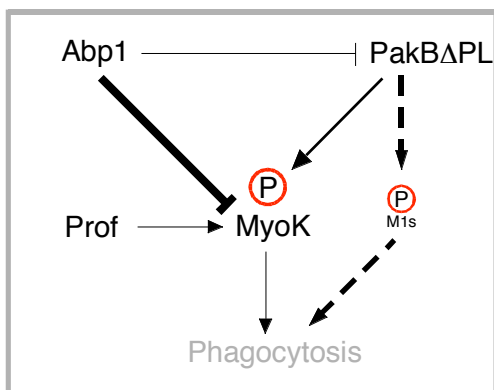
MyoK OE



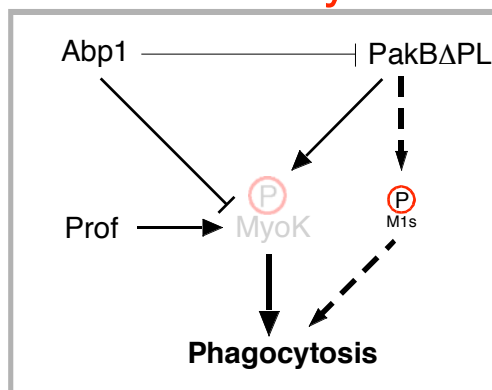
Abp1 OE



PakB Δ PL in wt



PakB Δ PL in MyoK null



>DDB0201562 |DDB_G0273447 |Protein| gene: abpE-1 on chromosome: 2 position 2984013 to 2985540

*MASLDISDPDITKYIKLVQDGNPANRWIVFSYVPKSNNKIKFCDSGSGDLKELREELDD
SSIRFAYIRFVINMMPKFVYIPWCGDGVNGPIKGAFIGHAIEFSKSFKPIHHQVNARSEE
DIDEKAITAALNKATGASYDSGSKVQGATKGTFI PQSVSQGREAAATKSNAEVKNVINKND
YNKIQESAEYWKQNQAN **KSEPAKPTR**PEYNLSTERDDYWKQQQAEKQKQQQQQQQASR
VNA **PPP**SRTVGNKFKQEQVSKPTETA **PPQPR**PAPSKGSVLNRFPAATQQQQE **PPAPSRPAA**
PVPSRVNKPAAPVQPVYQEPVHEEPQYEEPQYEE**PEE**EQQQQY**EE**QPT**EE**QQYY**QEE**PQQQY**E**
EQPT**EE**QQYY**QEE**EQQQY**EE**QPT**EE**QQYY**QEE**EQQQY**E**QPT**ED**QQYY**QEE**EQQQY**E**QPA**EE**QY
DQSGY **LQAKALYDYN**GENDG**DL**SFREGDIITILDQSDPDG**WW**Q**GS**LPT**GE**Q**GF**FPS**N**FVQ
QL*

ADF F-actin binding domain

Proline rich domain

SH3 binding motif (class I : **K/RxxPxxP**; classII : **PxxPxR**; minimal consensus sequence : **PxxP**)

Poly-Proline stretch

Acidic region

SH3 binding domain

>DDB0216177 |DDB_G0277849 |Protein| gene: dymA on chromosome: 3 position 252381 to 255025

MDQLIPVINKLQDVFNLTGSDPLDLPQIVVVGSSQSSGKSSVLENIVGRDFLPRGSGIVTR
RPLILQLTHLPIADDGSQTQEWGEFLHKPNDFYDFSEIREEIIIRDTRMTGKNKGISAQ
PINLKIYSPHVVNLTLDLPGITKVPVGDQPTDIEQQIRRMVMAYIKKQNAIIVAVTPAN
TDLANSDALQLAKEVDPEGKRTIGVITKLDLMDKGTDAMEVLTGRVIPLTLGFIGVINRS
QEDI IAKKSIRESLKSEILYFKNHPIYKS IANRSGTAYLSKTLNKL LMFHIRDTLPDLKV
KVS KMLSDVQGELSTYGDPLYDTKNSQGALLLQIITIFSSNFKDAIDGKLTDL SNNELYG
GARISYIFNEIYSHCVNNIDPLEGISLNDIRTTMRNATGPRAALFIPEISFELLVKKQVV
RLEEPSAQCV EYVYDELQRIVSQLEAKELSRFINLKARVIEVVNNLLQKHKVPTKTMIEH
LIKIETAFINTSHPDFVGGEGIFESLYKKQQLQQQNHLLQQLQDQYQQQQQQQQQQQQQNG
INNNQKGDNGNMNVNQQNMNQNMNQNSTNPFLOQQQQGQNKY **PGGPPA**QQQPNOQP
QLNKGPQNMPPNQSKPSSIPQNGPNNNNNNNNNNNRQDHQQGSFFSSFFRASPDPSLGQY
GGANNSNNSNN**PTSP**INSSSNSGNNYNTFGGQQSSSSSSQQLQSSQSQYKTSYNNNNNS
SSNNSYNRYQDDFYGRGDKLNQVPSIIKAPDDLTSKEKFETELIRELLISYFNIVKKNV
KDSVPKSI MHFLVNQSKEHIQNELVAALYKEELFDELLEESPQISSKRKSKAMIEILRK
ANEIINEIRDFRN*

Proline rich domain

SH3 binding motif (class I : **K/RxxPxxP**; classII : **PxxPxR**; minimal consensus sequence : **PxxP**)

ZPPφ (Z= P, G, A or a basic residue ; φ=hydrophobic)

Characteristic signature of the dynamin protein family:

- **GTP binding consensus sequences**
- GTP exchange domain